



Cite this: *RSC Adv.*, 2022, **12**, 16696

## Effect of chain extenders with different functionalities on the properties of single-component waterborne polyurethane ink binders<sup>†</sup>

Zhihui Yang and Xiang Cui  \*

Waterborne polyurethane (WPU) dispersions were prepared by post-chain extension and crosslinking reactions using 2-[(2-aminoethyl)-aminoethyl sulfonic acid sodium (AAS), diethylenetriamine (DETA), triethylenetetramine (TETA) and AAS/DETA as post-chain extenders, and their influence on the properties of WPUs was studied. Results showed the introduction of trifunctional DETA chain extenders significantly improved the molecular weight, T-peel strength, and water resistance of WPUs, suggesting that DETA was an effective crosslinking agent. The WPU dispersions with a 2 : 3 molar ratio of AAS/DETA chain extenders exhibited excellent properties. At a molar ratio of 1.6 for NCO groups to OH groups, a stable WPU dispersion possessed higher solid content of 42.8%. Furthermore, only 4 wt% organic solvents were used in the preparation of WPU dispersions. Results revealed that the obtained WPU dispersions are a potential candidate for binders in water-based inks, without removing organic solvents. This study may provide some insight or guidance for the design and preparation of water-based ink binders.

Received 28th April 2022

Accepted 26th May 2022

DOI: 10.1039/d2ra02707k

rsc.li/rsc-advances

### 1. Introduction

Volatile organic compounds are used in the preparation and applications of solvent-based inks, causing serious health, safety, and environmental problems.<sup>1,2</sup> Volatile solvents are the essential difference between water-based inks and solvent-based inks. Water-based inks are widely regarded as environmentally-friendly printing inks with high solid content, good gloss, and fluidity.<sup>3</sup> Binders are the most crucial part of water-based ink formulations that directly affects their properties, such as viscosity, adhesion, gloss, and drying time.<sup>4</sup>

Waterborne polyurethane (WPU) is an environmentally friendly material that has received increasing interest in a wide range of applications due to its unique structural features and intriguing properties.<sup>5-8</sup> WPU is used as a coating or adhesive in flexible packaging printing, especially as a binder in printing inks. Due to its environmental friendliness and simple preparation, WPU can significantly reduce the contamination caused by solvent-based inks.<sup>9,10</sup> In food packaging printing inks, boiling resistance is required, in addition to non-toxicity. Therefore, WPU ink binders should possess excellent adhesion properties.<sup>11</sup> However, most WPU products are linear polymers with relatively low average molecular weight, and some of their properties, such as water resistance, adhesion

strength, and mechanical properties are relatively poor and need significant improvement.<sup>12</sup>

Some properties of WPU products are improved by cross-linking modification.<sup>13,14</sup> Single-component and two-component cross-linking are the two most commonly used cross-linking methods. Although the two-component cross-linking technology can greatly improve the performance of WPU, the packaging, transportation, and use of the product are inconvenient, and their storage life is limited.<sup>15</sup> Compared with the two-component cross-linking technique, single component cross-linking has additional benefits and is widely used in research and applications. Single component chain extension cross-linking is performed during the preparation of WPU prepolymers (pre-extension cross-linking) and WPU water dispersion (post-extension cross-linking).<sup>16,17</sup> In general, the pre-extension cross-linking may significantly increase the viscosity of the WPU prepolymer, resulting in poor dispersion of the prepolymer in water. Therefore, organic solvent content is increased in the WPU prepolymer to reduce the viscosity of the system. However, the use of such organic solvents can harm the environment and human health.<sup>18,19</sup> Compared with pre-extension cross-linking approaches, post-extension cross-linking involves the addition of crosslinking agents when WPU prepolymer is dispersed in water, the viscosity of the prepolymer does not increase, and the prepolymer is easily dispersed in water without more organic solvent.

This work aimed to synthesize different WPU dispersions using a single-component post-chain extension cross-linking approach and to investigate the effects of chain extenders with different functionalities on the properties of WPUs. In

Department of Chemistry, Qinghai Normal University, Xining, 810008, P. R. China.  
E-mail: cui666kai@126.com; Tel: +86-971-6307635

† Electronic supplementary information (ESI) available. See <https://doi.org/10.1039/d2ra02707k>



addition to difunctional 2-[(2-aminoethyl)-amino]ethyl sulfonic acid sodium (AAS), multifunctional diethylenetriamine (DETA), triethylenetetramine (TETA), and AAS/DETA were also used as chain extenders for WPU synthesis. The molecular weight, average particle size, crystallization properties, thermal properties, dynamic mechanical properties, adhesion properties, and hydrophilic–hydrophobic properties of the prepared WPUs were investigated and related to chain extender structure.

## 2. Experimental

### 2.1 Materials

Poly( $\epsilon$ -caprolactone)diol (PCL,  $M_n = 2000$ , Wanhua, China) was dried at 90 °C *in vacuo* for 8 h before it was used. 1,4-Butanediol (BDO, Guangfu, China) was dried at 85 °C *in vacuo* for 4 h before it was used. Isophorone diisocyanate (IPDI, 98% purity, Aladdin), dimethylol propionic acid (DMPA, 99% purity, China),

triethylamine (TEA, AR grade, Lingfeng, China), diethylenetriamine (DETA, AR grade, Aladdin), triethylenetetramine (TETA, AR grade, Aladdin), 2-[(2-aminoethyl)-amino]ethyl sulfonic acid sodium (AAS, AR grade, Taiwan) and 1-methyl-2-pyrrolidinone (NMP, Lifeng, China) were used as received.

### 2.2 Synthesis of WPU dispersions

The synthesis scheme for WPUs is presented in Fig. 1. First, the WPU prepolymer was prepared. The free NCO content was 37.3 mol% (based on total NCO content). PCL and IPDI were added to a four-neck flask attached to a condenser, stirrer, and nitrogen flow port. The reaction temperature was controlled by a thermostated oil bath. The reaction mixture was heated at 85 °C and kept for 60 minutes at a 275 rpm stirring rate. DMPA then was added to the reaction system, and the mixture was reacted for another 90 minutes. The reaction temperature was

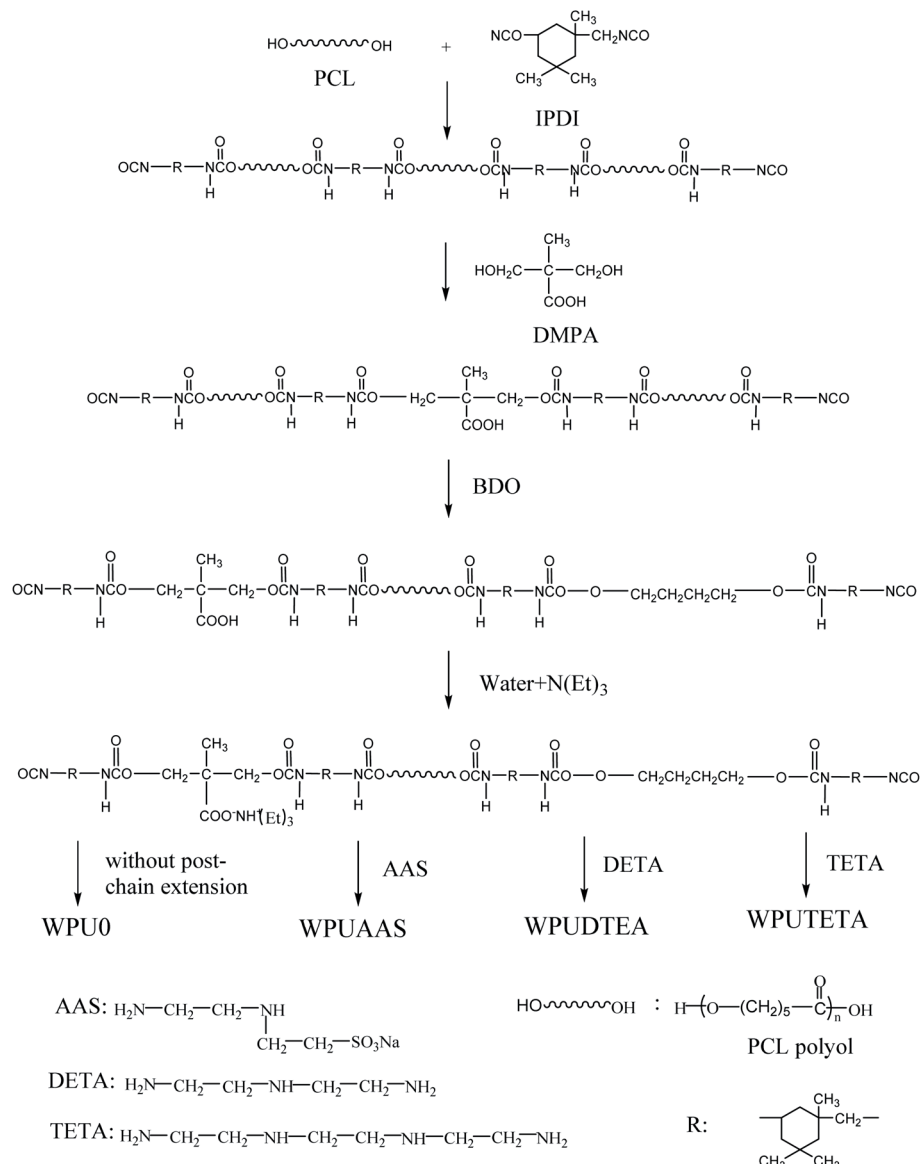


Fig. 1 Synthesis scheme of WPUs.



lowered to 75 °C and BDO was added to the flask. The reaction was continued for 90 minutes until the NCO content in the reaction system reached a predetermined value. The reaction temperature was again lowered to 50 °C, and then TEA was added to neutralize the carboxylic acid groups and obtain the WPU prepolymers. Throughout the reaction, NMP (4 wt% based on total WPU dispersions) was added to the flask to adjust the viscosity of the reaction mixture. The infrared spectra of the WPU prepolymer are shown in Fig. S1.† The absorption peak at 2270 cm<sup>-1</sup> was attributed to the free NCO groups in IPDI, suggesting that the NCO groups in the prepolymer did not react completely.

Secondly, the WPU dispersions were prepared. The desired amount of deionized water was added to the prepared prepolymers and dispersed at a stirring speed of 1000 rpm at 35 °C. Then, the AAS, DETA, TETA, and composite AAS/DETA chain extenders were separately added to the above dispersions to prepare four WPU dispersions, respectively. Solid contents of WPU dispersions were about 40 wt%. To study the effects of different chain extenders on the properties, WPU dispersions without chain extenders were also prepared and referred to as WPU0. WPU samples prepared with AAS, DETA, or TETA chain extender are referred to as WPUAAS, WPUDETA, and WPUTETA, respectively. Table 1 lists the basic formulation for the preparation of WPUs.

### 2.3 Preparation of WPU films

The prepared WPU dispersions were poured into a tetrafluoroethylene mold. The dispersions were dried at room temperature for 24 hours and then under vacuum for another 24 hours until the WPU films reached a constant weight. The dried WPU films (about 1 mm thick) were stored for later use.<sup>20,21</sup>

### 2.4 Material characterization

**2.4.1 Fourier transform infrared spectroscopy (FTIR).** The chemical structure of the WPU films was analyzed using FTIR (IS50, Nicolet, USA) at a resolution of 4 cm<sup>-1</sup>. Data were averaged over 32 scans and were collected in total reflection mode.<sup>22</sup>

**2.4.2 X-ray diffraction.** The crystallization properties of the WPU films were analyzed with X-ray diffraction (Bruker,

Germany). Data were collected at scattering angles,  $2\theta$ , between 5 and 60° using a scan speed of 4° min<sup>-1</sup>.<sup>3</sup>

**2.4.3 Differential scanning calorimetry (DSC).** The thermal properties of the WPU films were analyzed using a differential scanning calorimeter (PerkinElmer, USA). Approximately 5–10 mg of the WPU film samples were sealed in an aluminum crucible under nitrogen. The first heating ramp was performed at a heating rate of 10 °C min<sup>-1</sup> over a temperature range from 25–135 °C. The first cooling step was performed at a rate of 5 °C min<sup>-1</sup> over a temperature range from 135 to –70 °C. The second heating ramp was performed at a rate of 10 °C min<sup>-1</sup>, and the temperature range was –70 to 135 °C.<sup>3</sup>

**2.4.4 Dynamic mechanical properties (DMA).** The dynamic mechanical properties of the WPU films were analyzed using a dynamic mechanical analyzer (Netzsch 242E, Germany) at a frequency of 1 Hz, a heating rate of 5 °C min<sup>-1</sup>, and over a temperature range of –70 to 100 °C.<sup>22</sup>

**2.4.5 Gel permeation chromatography (GPC).** The molecular weights of the WPU samples were determined using gel permeation chromatography (PL-GPC50, UK). Samples for GPC were prepared by dissolving the WPU films in tetrahydrofuran (THF) at a concentration of 0.1%. For GPC measurements, the THF flow rate was 1.0 ml min<sup>-1</sup>, and the sample injection volume was 10 μL.<sup>3</sup>

**2.4.6 T-peel strength.** The T-peel strengths of the WPU films were measured using an electronic tensile tester (BLD-200H, China). The tests were carried out at a temperature of 23 ± 2 °C and relative humidity of 50 ± 5% using a 90° angle and a crosshead speed of 300 mm min<sup>-1</sup>. The prepared WPU films were first coated on a poly terephthalate (PET) film, then coated with a polyurethane adhesive, and finally laminated with a castable polypropylene (CPP) film to obtain the laminated film samples<sup>11</sup> as illustrated in Fig. 2.

**2.4.7 Storage stability.** To determine the storage stability of the dispersions, 50 ml of the WPU dispersions were added to a glass bottle and sealed with a lid at room temperature. The appearance and morphology of the dispersions were observed every day. The storage stability was defined as the day when gel and precipitates appeared in the dispersions.<sup>23</sup>

**2.4.8 Boiling resistance.** Boiling resistance was measured according to Chinese Standard GB/T 10004-2008. The prepared

Table 1 Basic formulation for the preparation of WPUs

Preparation method	Raw materials	Content (g)	Degree of chain extender <sup>a</sup> (%)
WPU prepolymer	IPDI	10.24	
	PCL	25.01	
	DMPA	1.01	
	BDO	0.8	
	TEA	0.76	
Post-extension cross-linking	AAS	Calculated according to the degree of chain extender	0–100 <sup>b</sup>
	DETA		60
	TETA		60
	AAS/DETA		60

<sup>a</sup> The degree of chain extender was defined as the molar percentage of amino groups in the chain extender compared to the theoretically remaining amount of NCO groups in the WPU prepolymer. <sup>b</sup> The degree of chain extender was 0, 20%, 40%, 60%, 80%, 100%.





Fig. 2 Schematic diagram of PET/CPP laminate film samples for the measurements of T-peel.

laminate films (Fig. 2) were heat sealed to create test bags, and the test bags were boiled in water at 121 °C for 30 minutes and the observed was determined.

Standard deviation (SD) error bars were used to show statistical analysis of data results in this study. SD was calculated by the following formula;<sup>24</sup>

$$SD = \sqrt{\frac{\sum (X - M)^2}{n - 1}}$$

where  $X$  refers to a single data point,  $M$  is the mean, and  $\sum$  (sigma) indicates the sum, for all  $n$  data points.

### 3. Results and discussion

#### 3.1 Degree of chain extension of WPUs

Chain extension and crosslinking increase the molecular weight of WPUs. Therefore, changes in WPU molecular weight reflect the degree of chain extension. GPC is used to analyze the number-average molecular weight ( $M_n$ ), weight-average molecular weight ( $M_w$ ), and polydispersity index (PDI) of WPUs. Fig. 3 shows the  $M_n$  and  $M_w$  of WPUs at different degrees of chain extension using AAS as the chain extenders.

It can be seen that both  $M_n$  and  $M_w$  of the WPUs first rapidly increased and then plateaued with an increase in the degree of chain extension. The molecular weight did not increase significantly with further degrees of chain extension above 60%, suggesting that the maximum degree of chain extension

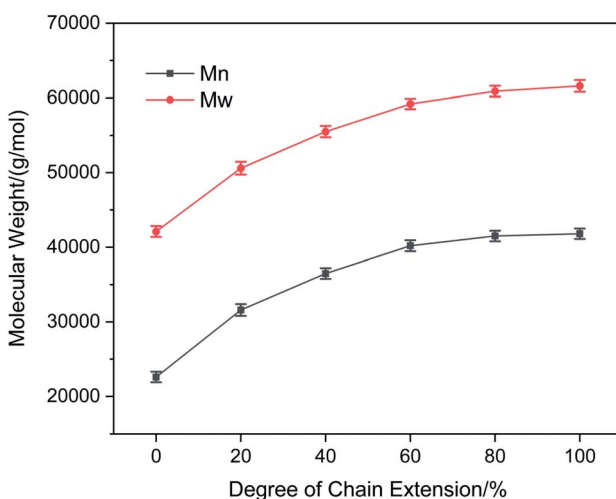


Fig. 3  $M_n$  and  $M_w$  of WPUs at different degrees of chain extension using AAS as chain extenders. For each case, the error bars show SD ( $n = 3$ ).

achieved in this study was about 60%. This result suggested that not all the remaining NCO groups on the latex particles could react with the chain extenders, possibly because some of the NCO groups were located inside the colloidal particles and therefore could not participate in the post-chain extension reaction.

#### 3.2 Influence of chain extenders with different functionalities on the properties of WPUs

In this study, the degree of chain extension was fixed at 60%, and the influences of different functional chain extenders, such as AAS, DETA, and TETA, on the properties of WPUs were investigated.

**3.2.1 Average particle size of the WPU dispersions.** In general, smaller average particle sizes correspond to higher densities of particles in WPU dispersions, leading to an increase in the surface-to-volume ratio and allowing more reactions to take place at the particle surface.<sup>25,26</sup> As a result, more NCO groups on the surface of colloidal particles reacted with amino groups in chain extenders, thereby, increasing the degree of chain extension. In this study, all dispersions were prepared from the same WPU prepolymer under the same synthesis conditions, and average particle sizes and residual NCO group contents were the same before the crosslinking reactions. Fig. 4 shows the effects of chain extenders with different functionalities on the average particle size of WPU dispersions. The average particle size of WPUAAS, WPUTETA, and WPUTETA was larger than that of WPU0, indicating that the post-extension cross-linking reactions mainly occurred on the surface of dispersed WPU latex particles.<sup>27,28</sup> The highest particle size and particle size distribution were seen in the WPUTETA sample, suggesting that DETA had a higher degree of reaction that promotes the aggregation of WPU latex particles. This was attributed to multiple amino groups in the DETA molecular chain that reacted with NCO groups on the surface of different colloidal particles, thereby, increasing the size of particles.

**3.2.2 Chemical structure of WPU films.** Fig. 5 shows infrared spectra of different WPU films. IR curves of different

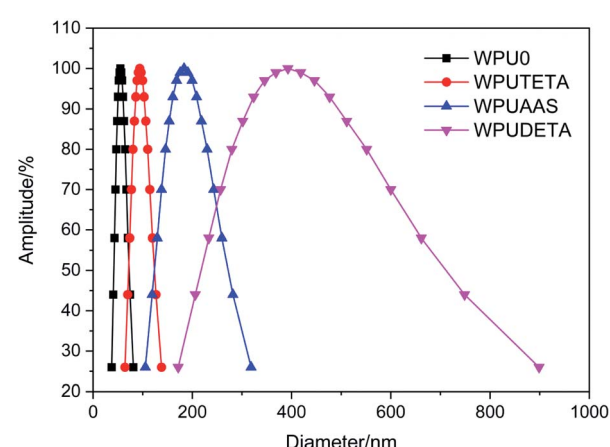


Fig. 4 The effect of chain extenders with different functionalities on the average particle size of WPU dispersions.



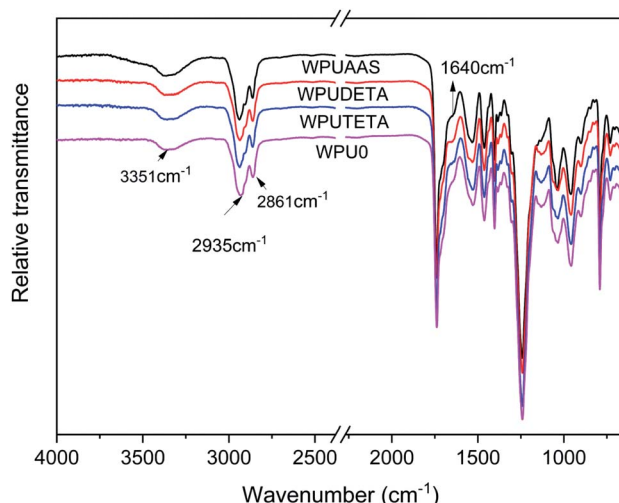


Fig. 5 Infrared spectra of WPU films with different functional chain extenders.

WPU films were very similar. The free N–H stretching vibrations was observed between 3447–3600  $\text{cm}^{-1}$ ; however, the N–H stretching vibration measured for WPU films shifted to 3351  $\text{cm}^{-1}$ , indicating the formation of hydrogen between the N–H and C=O groups. C–H absorption peaks were observed at 2935  $\text{cm}^{-1}$  and 2861  $\text{cm}^{-1}$ . The absorption peak at around 1640  $\text{cm}^{-1}$  was assigned to the ordered hydrogen-bonded urea carbonyl, and the peak intensity for the WPUDETA sample was the highest among the four WPU samples. This was attributed to the reaction between amino groups in the chain extenders with the remaining NCO groups in WPU prepolymers, forming more polar urea groups.

**3.2.3 Molecular weight of WPU films.** Fig. 6 shows the effect of chain extenders with a degree of chain extension of 60% on  $M_n$  and  $M_w$  of WPU films. Table 2 lists the relevant GPC analysis data. Results showed that compared with WPU without

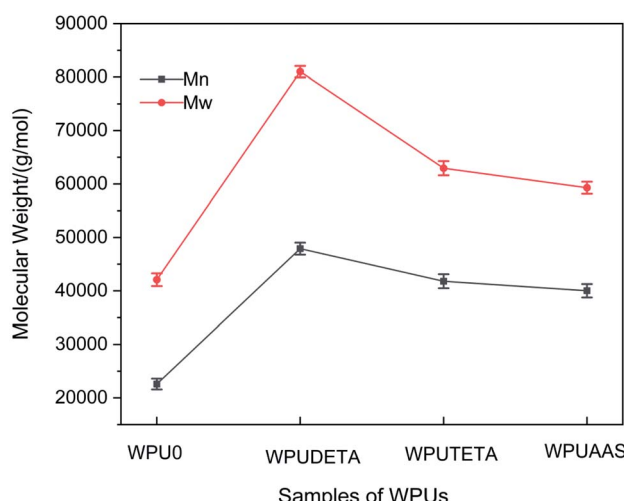


Fig. 6 The effect of chain extenders with different functionalities at a 60% degree of chain extension on  $M_n$  and  $M_w$  of WPU films. For each case, the error bars show SD ( $n = 3$ ).

Table 2 GPC analysis data of WPU films with different functional chain extenders at a 60% degree of chain extension

Sample	$M_n$	$M_w$	PDI ( $M_w/M_n$ )
WPU0	22 610	42 101	1.86
WPUDETA	47 913	81 014	1.69
WPUTETA	41 802	62 947	1.51
WPUAAS	40 210	59 276	1.48

chain extension, the molecular weight of WPU prepared with post-chain extension increased. In addition, the multifunctional DETA and TETA reacted with WPU prepolymer to form three-dimensional cross-linked structures, thereby, increasing the molecular weights of WPUDETA and WPUTETA samples more than that of WPUAAS sample. The molecular weight of WPUDETA was higher than that of WPUTETA, indicating that the degree of reaction with the DETA chain extenders was higher than that of TETA chain extenders. Moreover, three WPU samples with post-chain extenders showed very close PDI (polydispersity index) value (ranging from 1.48 to 1.69), indicating that the chain extenders with different functionalities affected the polydispersity only to a limited extent.

**3.2.4 Crystallization properties of WPU films.** Fig. 7 shows X-ray diffraction patterns of neat PCL and WPU films. The neat PCL exhibited two prominent peaks at 21.48° and 23.8°, attributed to (110) and (200) plane diffraction of PCL soft segments, respectively.<sup>29</sup> However, WPUs exhibited a broad diffraction peak near 19.8° with relatively weak intensities compared to pure PCL. This indicated that the hard segments and chain extension reaction hindered the crystallization of PCL soft segments. In addition, all WPU films showed two weaker diffraction peaks near 30°, similar to pure PCL, suggesting that these two peaks were formed due to the crystallization of PCL soft segments. Among all WPU samples, the intensity of the main diffraction peak of WPUDETA was the weakest (below 600). Compared with other chain extenders, DETA showed a higher degree of cross-linking reaction that, restricted the chain segment movements and disrupted the regular ordering of chain segments, thereby, decreasing the crystallization of soft segments.

**3.2.5 Thermal properties of WPU films.** Fig. 8 shows DSC thermograms of WPU films with different functional chain extenders. The glass transition temperature of soft segments ( $T_g$ s) ranged from  $-37.5$  to  $-34.7$  °C in all samples. No endothermic melting peaks were detected, indicating that the crystallization was very slow.<sup>30</sup> In addition, the  $T_g$ s were almost the same, due to the same soft segment contents in all WPUs.

**3.2.6 Dynamic mechanical properties of WPU films.** Dynamic mechanical properties of WPU films were studied by DMA. Fig. 9 shows the variation in the storage modulus, loss modulus, and tan delta of WPU films with different functional chain extenders as a function of temperature. When the temperature was lower than  $-37$  °C, the storage modulus of four WPU films was almost unchanged, indicating that these films were in a glass state. After passing through the glass transition region, the storage modulus of all samples showed



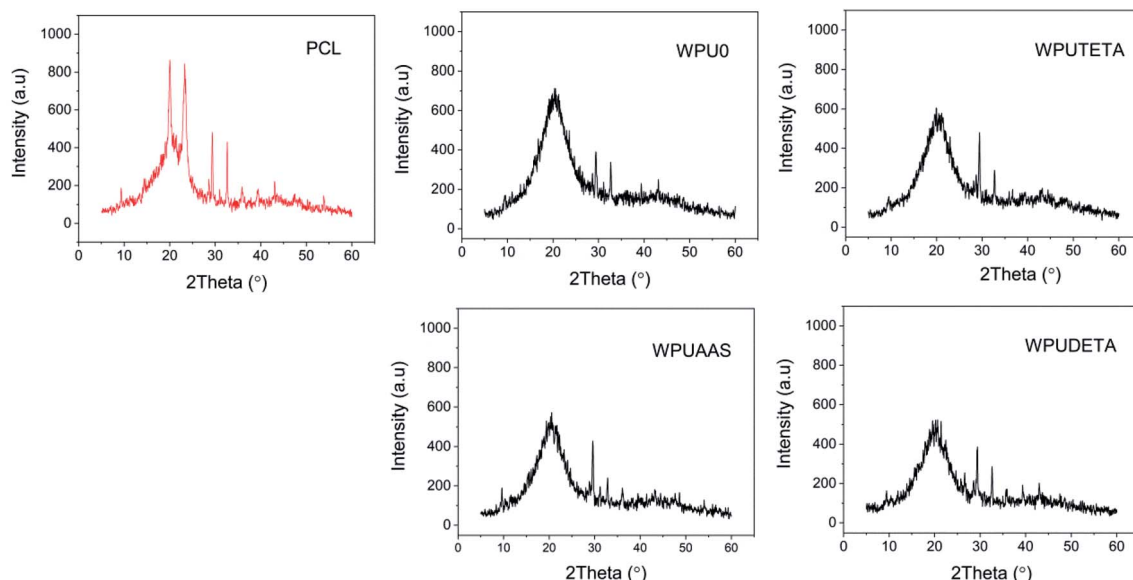


Fig. 7 X-ray diffraction pattern of neat PCL and WPU films.

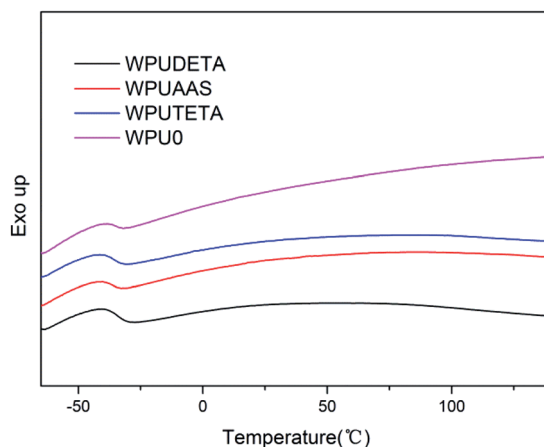


Fig. 8 DSC thermograms of WPU films with different functional chain extenders.

a significant decline due to the amorphous structure of WPUs. The decline in storage modulus corresponded to the major relaxation process associated with the glass–rubber transition.<sup>31</sup> Among four WPU films, WPUDETA exhibited the fastest drop rate, due to the formation of more polar urea bonds and interchain hydrogen bonds between the macromolecular chains in the cross-linked WPUDETA films, which disordered the polyurethane chain structures and decreased the crystallinity.<sup>32</sup> Fig. 9(b) and (c) indicate that the transition peak between  $-45\text{ }^{\circ}\text{C}$  and  $-15\text{ }^{\circ}\text{C}$  belonged to  $T_{\text{g}}\text{s}$ . Another transition peak between  $45\text{ }^{\circ}\text{C}$  and  $90\text{ }^{\circ}\text{C}$  corresponded to the glass transition temperature of the hard segment ( $T_{\text{g}}\text{h}$ ). Except for WPU0, both  $T_{\text{g}}\text{s}$  and  $T_{\text{g}}\text{h}$  of the other three chain extension cross-linked WPUs were observed. The difference between  $T_{\text{g}}\text{h}$  and  $T_{\text{g}}\text{s}$ ,  $\Delta T_{\text{g}} = T_{\text{g}}\text{h} - T_{\text{g}}\text{s}$ , was related to the degree of microphase separation between soft and hard segments in WPU films.  $T_{\text{g}}$  and  $\Delta T_{\text{g}}$

values obtained from DMA curves are listed in Table 3.  $T_{\text{g}}\text{s}$  values measured with DSC and DMA were slightly different due to the different measurement principles of the two methods, relatively close overall. Among three WPU films that were prepared with a post-chain extension step, the  $\Delta T_{\text{g}}$  ( $102.5\text{ }^{\circ}\text{C}$ ) of WPUDETA was the largest, indicating the degree of phase separation between hard and soft segments was the largest in this sample. Since the higher crosslinking density in WPUDETA films limited the molecular chain movements, these WPU films showed the highest  $T_{\text{g}}\text{h}$  value compared to other WPU sample films.

**3.2.7 T-peel strength of WPU films.** The adhesion properties of WPU films were evaluated by the T-peel strength test. Fig. 10 shows the T-peel strength values of WPU films with different functional chain extenders. The T-peel strength for WPUAAS, WPUDETA, and WPUTETA were all higher than that of WPU0, indicating that the post-chain extension crosslinking reaction improved the adhesion strength of WPU films. Amino groups in chain extenders reacted with NCO groups on the particle surfaces to form polar urea groups, which enhanced the interactions between WPU particles, WPU particles, and PET films. In addition, WPUDETA films demonstrated the greatest T-peel strength value, correlated with the highest crosslink density in this sample.

**3.2.8 Surface property of WPU films.** Water absorption, contact angle, and surface energy are three important physical parameters affecting the type of application of WPUs.<sup>33,34</sup> The water absorption and water contact angle measurements were used to evaluate the hydrophilic–hydrophobic properties of WPU films. It is recognized that WPU films were hydrophilic and wettable when the water contact angle was less than  $90\text{ }^{\circ}$ .<sup>35,36</sup> Fig. 11(a) and (b) show water contact angle measurements and water absorption rates of different WPU films, respectively, and the relevant data are listed in Table 4. Results revealed that the water contact angle increased according to WPU0  $\text{<} \text{ WPUTETA} \text{ <} \text{ WPUDETA}$ .



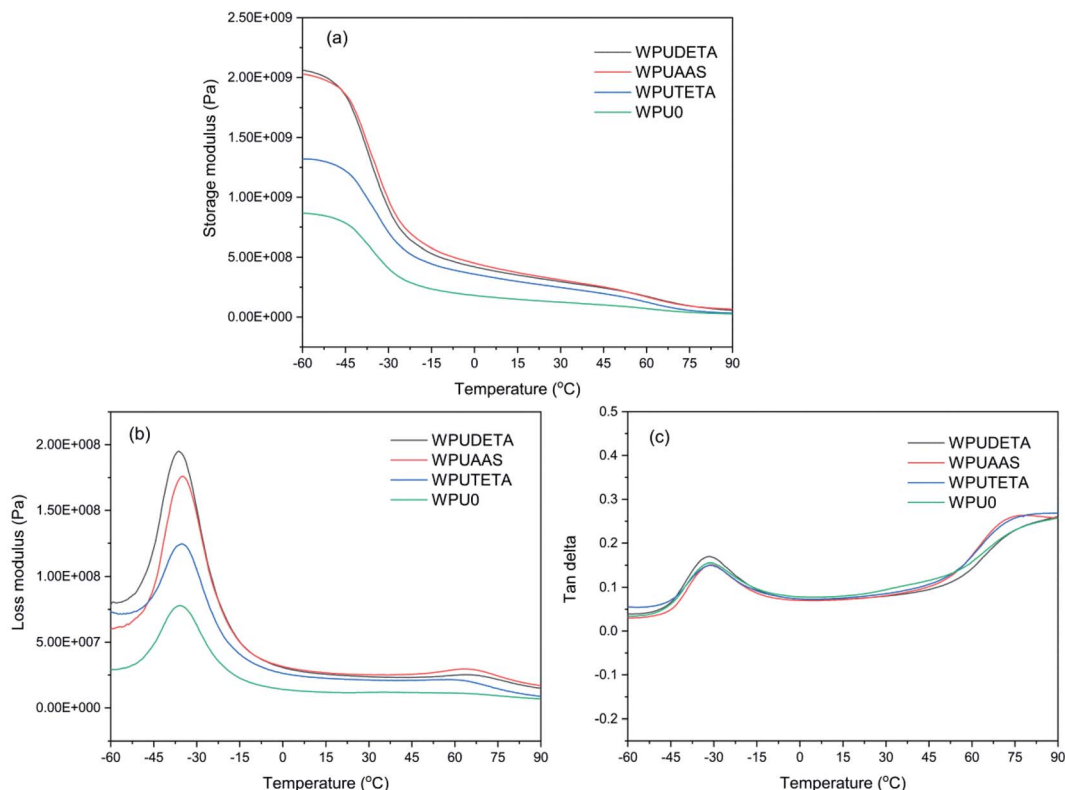


Fig. 9 Storage modulus (a), loss modulus (b), and tan delta (c) of WPU films with different functional chain extenders.

Table 3  $T_g$  and  $\Delta T_g$  values obtained from DMA curves

Sample	WPU0	WPUAAS	WPUDETA	WPUTETA
$T_g^s$ (°C)	-35.8	-33.9	-36.2	-34.9
$T_g^h$ (°C)	—	64.9	66.3	61.9
$\Delta T_g$ (°C)	—	98.8	102.5	96.8

WPUAAS < WPUDETA, while the trend in the water absorption rate was the opposite. WPUDETA showed a higher water contact angle (90°) and a lower water absorption rate (8.1%). This shows

that WPUDETA films had better hydrophobicity compared to the other three WPU samples.

To further study the surface properties of WPU films, the surface energy of all samples was calculated using static contact angles of ethylene glycol and water following eqn (1) and (2).<sup>37-39</sup>

$$\gamma_L(1 + \cos \theta) = 4 \left( \frac{\gamma_s^d \gamma_L^d}{\gamma_s^d + \gamma_L^d} + \frac{\gamma_s^p \gamma_L^p}{\gamma_s^p + \gamma_L^p} \right) \quad (1)$$

$$\gamma_s = \gamma_s^d + \gamma_s^p \quad (2)$$

where  $\gamma_L$  and  $\gamma_s$  are the surface tension of liquid and surface energy of solid, respectively.  $\gamma_L^d$  and  $\gamma_s^d$  are dispersion components of  $\gamma_L$  and  $\gamma_s$ ,  $\gamma_L^p$  and  $\gamma_s^p$  are polar components of  $\gamma_L$  and  $\gamma_s$ . Dispersion components of water and ethylene glycol are 21.8 mJ m<sup>-2</sup> and 29.3 mJ m<sup>-2</sup>, respectively, and their polar components are 51.0 mJ m<sup>-2</sup> and 19.0 mJ m<sup>-2</sup>, respectively.

Surface energy is one of the important parameters in evaluating the water and oil repellence of WPU. Generally, WPU films with relatively low surface energy have favorable water and oil repellence.<sup>40,41</sup> As presented in Table 4, WPUDETA had the smallest surface energy (27.02 mJ m<sup>-2</sup>) among four samples, revealing its best water and oil repellence properties. This might be attributed to the higher chain stiffness of WPUDETA films restricting the hydrophilic groups from reaching the particle surface. As a result, the hydrophilicity of the WPU film's surface was reduced, and the surface energy was also reduced at the same time.<sup>40,42</sup> Therefore, WPUDETA had lower surface energy and better water and oil resistance compared to other samples.

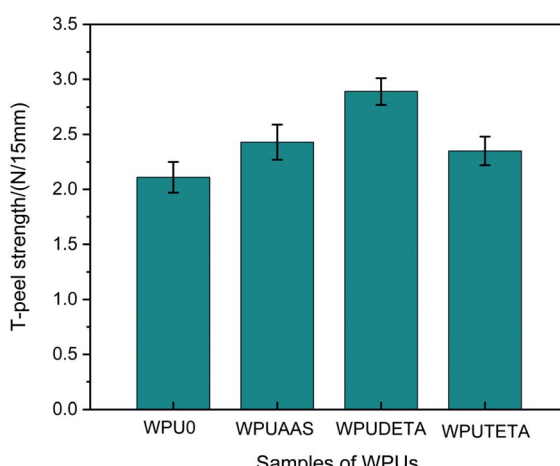


Fig. 10 T-peel strength values of WPU films with different functional chain extenders. For each case, the error bars show SD ( $n = 3$ ).



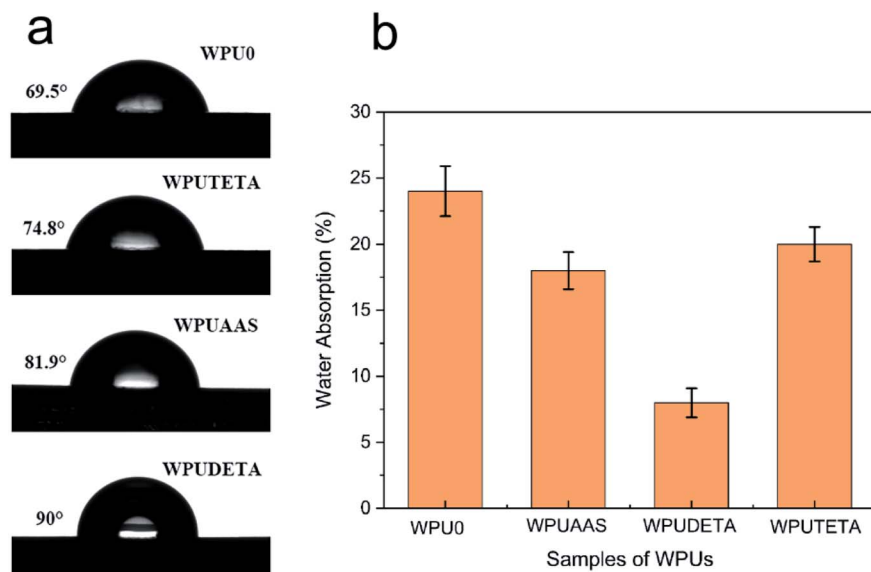


Fig. 11 Photos of water contact angles (a) and water absorption rates (b) of WPU films with different functional chain extenders. For each case, the error bars show SD ( $n = 3$ ).

Table 4 Water absorption, contact angle, and surface energy data for WPU films

Sample	Water absorption (%)	Contact angle (°)		Surface energy (mJ m <sup>-2</sup> )		
		H <sub>2</sub> O	(CH <sub>2</sub> OH) <sub>2</sub>	$\gamma_s^p$	$\gamma_s^d$	$\gamma_s$
WPU0	24.2	69.5	45.2	16.18	21.82	38.00
WPUAAS	18.4	81.9	58.1	15.01	15.47	30.48
WPUDETA	8.1	90	64.2	16.27	10.75	27.02
WPUTETA	20.5	74.8	54.2	13.60	20.44	34.04

### 3.3 Properties of WPU prepared with the AAS/DETA compound chain extenders

**3.3.1 Influence of AAS/DETA molar ratio on the properties of WPUs.** The above results show that the WPUDETA had higher molecular weight, better adhesion strength, and water and oil resistance. Therefore, DETA was considered an effective chain extender that significantly improved the WPU properties. However, if DETA was the only chain extension crosslinking

agent, then the storage stability of the WPU dispersions would likely be lower due to the excessive degree of cross-linking between the particles. Therefore, AAS and DETA were used as compound chain extenders to prepare a series of WPUs. At the same time, the influence of the AAS/DETA molar ratio ( $n$ ) on the properties of WPUs was investigated, and the results are summarized in Table 5. As the DETA content increased, the average particle size increased while the storage stability of WPU dispersions decreased, and the dispersion appearance also changed from transparent to translucent, and then to milky white. Meanwhile, the boiling resistance and water resistance of WPU films gradually improved with higher DETA contents. Besides, the gloss and light transmittance of WPU films did not change much with the increase in DETA content, indicating that the type and composition of chain extenders have little effect on WPU gloss and light transmittance. When the molar ratio of AAS to DETA was 2 : 3, the WPU films possessed a higher T-peel strength value (3.03 N/15 mm). The WPU with a molar ratio of 2 : 3 for AAS/DETA showed excellent comprehensive properties.

**3.3.2 Influence of NCO/OH molar ratio on the properties of WPUs.** WPU dispersions prepared with low organic solvent

Table 5 Properties of WPUs prepared with different AAS/DETA molar ratios<sup>a</sup>

$n$ (AAS : DETA)	1 : 0	4 : 1	3 : 2	2 : 3	1 : 4	0 : 1
Appearance	Transparent	Transparent	Transparent	Transparent	Translucent	Milky white
Particle size (nm)	183.3	194.5	198.1	207.4	286.4	392.2
Gloss (60°)	80	81	79	78	74	72
Light transmittance (%)	85	87	84	82	79	78
Water resistance	+	++	++	+++	+++	+++
T-peel strength (N/15 mm)	2.43	2.62	2.84	3.03	2.95	2.89
Boiling resistance	+	+	++	+++	+++	+++
Storage stability	>6 months	>6 months	>6 months	>6 months	>5 months	>4 months

<sup>a</sup> +++ best; ++ good; + worst.



Table 6 Influence of NCO/OH molar ratio on the properties of WPUs<sup>a</sup>

NCO/OH	1.3	1.4	1.5	1.6	1.7
Appearance	Transparent	Transparent	Transparent	Transparent	Milky white
Particle size (nm)	122.1	162.8	181.3	194.6	246.9
Solid content (%)	35.2	36.5	39.6	42.8	39.4
Boiling resistance	+++	+++	+++	+++	++
Storage stability	>6 months	>6 months	>6 months	>6 months	>4 months

<sup>a</sup> +++ best; ++ good; + worst.

contents (4 wt% based on total WPU dispersions) do not require the removal of organic solvents and avoid the need for a solvent recovery step, facilitating the industrial production of such WPU dispersions. To prepare stable WPU dispersions with low organic solvent contents and high solids contents, the viscosity of the WPU prepolymer must be reduced. The NCO/OH molar ratio is a key factor in determining the viscosity of WPU prepolymers, whereas prepolymers with high NCO/OH molar ratios have lower molecular weights and viscosities.<sup>43</sup> The influence of the NCO/OH molar ratio on the properties of WPUs prepared is shown in Table 6. Obtained results showed that as the NCO/OH molar ratio increased from 1.3 to 1.7, the average particle size increased from 122.1 nm to 246.9 nm, the appearance of the solution changed from transparent to milky white, solid contents increased from 35.2% to 42.8% and then decreased to 39.4%. WPU prepolymers with lower NCO/OH molar ratios had larger molecular weights and viscosities, and more water was needed to disperse the WPU prepolymer, enabling WPU dispersions to have lower solids content. As the NCO/OH molar ratio increased, both molecular weight and viscosity of the WPU prepolymer gradually decreased, water required to disperse the prepolymer decreased, and solid contents of the WPU dispersions increased. When the NCO/OH molar ratio increased from 1.6 to 1.7, the WPU solid contents decreased from 42.8% to 39.4%. When the molar ratio of NCO/OH increased to 1.7, more remaining NCO groups reacted with water to produce more hydrophobic urea groups, making the dispersion of WPU prepolymer in water more difficult and decreasing the solid contents. In addition, after the chain extension reaction, the residual NCO groups reacted with amine groups in the chain extender which increased the degree of entanglement between the polyurethane chains on the surface of WPU particles, thereby, increasing the particle size and decreasing the storage stability of dispersions. WPU dispersions prepared with a molar ratio of NCO groups to OH groups of 1.6 had higher solid content and better storage stability.

## 4. Conclusions

A series of WPUs were prepared using different functional chain extenders. The influences of chain extenders type on the properties of WPUs were investigated. The average particle size of WPU dispersions with post-chain extenders was larger than that of WPUs without chain extension. Results showed that the post-chain extension reaction mainly occurred on the surface of colloidal particles. The molecular weight of WPUs did not

increase significantly above a degree of chain extension of 60%, indicating that the maximum effective degree of chain extension was about 60%. Compared with other WPUs, the WPU prepared by the DETA crosslinker showed higher  $M_n$ ,  $M_w$ , and T-peel strength, about 47 235 g mol<sup>-1</sup>, 81 141 g mol<sup>-1</sup>, and 2.89 N/15 mm, respectively. In addition, it had lower water absorption and surface energy of 8% and 27.02 mJ m<sup>-2</sup>, respectively. These results indicated that the trifunctional DETA was an effective crosslinking modifier to improve WPUs' properties. The best comprehensive properties were observed for WPUs prepared with a composite AAS/DETA crosslinker at a 2 : 3 molar ratio and the corresponding WPU films had higher T-peel strength of 3.03 N/15 mm. The use of both carboxylate and sulfonate hydrophilic chain extenders to prepare WPUs with a molar ratio of NCO/OH of 1.6 reduced the viscosity of WPU prepolymers, and the obtained stable dispersions had a higher solid content of 42.8% using only 4 wt% of organic solvent in the preparation process, thereby, avoiding the costs associated with removing organic solvents. In addition, this is beneficial to the industrial-scale production of these materials.

## Conflicts of interest

There are no conflicts to declare.

## Acknowledgements

Financial support from the Applied Basic Research Project of Science and Technology Department from Qinghai province (Grant number 2020-ZJ-729) is acknowledged.

## References

- 1 X. Zhou, Y. Li, C. Fang, S. J. Li, Y. L. Cheng, W. Q. Lei, *et al.*, *J. Mater. Sci. Technol.*, 2015, **31**, 708–722.
- 2 Y. Zhang, W. B. Zhang, X. Wang, Q. W. Dong, X. Y. Zeng, R. L. Quirino, *et al.*, *Prog. Org. Coat.*, 2020, **142**, 105588.
- 3 J. T. Zhu, Z. M. Wu, D. Xiong, L. S. Pan and Y. J. Liu, *Prog. Org. Coat.*, 2019, **133**, 161–168.
- 4 R. Maria and F. Andrew, *Prog. Org. Coat.*, 2006, **57**, 183–194.
- 5 Y. Fang, X. Du, X. Cheng, M. Zhou, Z. Du and H. Wang, *Polymer*, 2020, **15**, 188–195.
- 6 G. Wu, D. Liu, J. Chen, G. Liu and Z. Kong, *Prog. Org. Coat.*, 2019, **127**, 80–87.
- 7 I. J. Gomez, J. Wu, J. A. Roper, H. Beckham and J. C. Meredith, *ACS Appl. Polym. Mater.*, 2019, **1**, 3064–3073.



8 K. P. Wang, Y. P. Deng, T. Wang, Q. D. Wang, C. G. Qian and X. Y. Zhang, *Polymer*, 2020, **210**, 123017.

9 G. Zheng, M. Lu and X. Rui, *Appl. Surf. Sci.*, 2017, **399**, 272–281.

10 W. Song, B. Wang, L. Fan, F. Ge and C. Wang, *Appl. Surf. Sci.*, 2019, **463**, 403–411.

11 L. Lei, Z. B. Xia, C. B. Ou, L. Zhang and L. Zhong, *Prog. Org. Coat.*, 2015, **88**, 155–163.

12 Z. Liang, J. T. Zhu, F. Q. Li, Z. M. Wu, Y. J. Liu and D. Xiong, *Prog. Org. Coat.*, 2021, **150**, 105972.

13 K. Hyelin, L. Younghee, K. Jungsoo, P. C. Cheol, H. Park, C. H. Wan, *et al.*, *J. Polym. Res.*, 2016, **23**, 240.

14 X. Cao, X. Ge, H. Chen and W. Li, *Prog. Org. Coat.*, 2017, **107**, 5–13.

15 X. Zhu, Q. Zhang, L. Liu, X. Z. Kong and S. Feng, *Prog. Org. Coat.*, 2007, **59**, 324–330.

16 J. J. Li, W. Zheng, W. B. Zeng, D. Q. Zhang and X. H. Peng, *Appl. Surf. Sci.*, 2014, **307**, 255–262.

17 M. M. Rahman, *J. Adhes. Sci. Technol.*, 2013, **27**, 2592–2602.

18 Y. Nomura, A. Sato, S. Sato, H. Mori and T. Endo, *J. Polym. Sci., Part A: Polym. Chem.*, 2007, **45**, 2689–2704.

19 B. Vogt-Birnbrich, *Prog. Org. Coat.*, 1996, **29**, 31–38.

20 D. D. Li, D. G. Hu, J. H. Tan, Q. H. Zhu, Z. L. Liu, C. Su, *et al.*, *Mater. Des.*, 2021, **211**, 110142.

21 Q. Yu, P. T. Pan, Z. L. Du, X. S. Du, H. B. Wang and X. Cheng, *RSC Adv.*, 2019, **9**, 7795.

22 M. W. Dai, J. Y. Wang and Y. Zhang, *Colloids Surf. A Physicochem. Eng. Asp.*, 2020, **601**, 124994.

23 L. j. Hou, Y. T. Ding, Z. L. Zhang, Z. S. Sun and Z. H. Shan, *Colloids Surf. A Physicochem. Eng. Asp.*, 2015, **467**, 46–56.

24 G. Cumming, F. Fidler and D. L. Vaux, *J. Cell Biol.*, 2007, **177**(1), 7–11.

25 J. Wu and P. T. Mather, *Polym. Rev.*, 2009, **49**, 25–63.

26 C. P. Whitby and R. Parthipan, *J. Colloid Interface Sci.*, 2019, **554**, 315–323.

27 Y. K. Jhon, I. W. Cheong and J. H. Kim, *Colloids Surf. A Physicochem. Eng. Asp.*, 2001, **179**, 71–78.

28 J. Yoon Jang, Y. Kuk Jhon, I. Woo Cheong and J. Hyun Kim, *Colloids Surf. A Physicochem. Eng. Asp.*, 2002, **196**, 135–143.

29 Q. Meng, J. Hu and S. Mondal, *J. Membr. Sci.*, 2008, **319**, 102–110.

30 M. Pérez-Limiñana, F. Aran-Ais, A. M. Torró-Palau, A. César Orgilés-Barceló and J. Miguel Martín-Martínez, *Int. J. Adhes. Adhes.*, 2005, **25**, 507–517.

31 M. A. S. Azizi Samir, F. Alloin, J. Y. Sanchez and A. Dufresne, cross-linked nanocomposite polymer electrolytes reinforced with cellulose whiskers, *Macromolecules*, 2004, **37**, 4839–4844.

32 P. Florian, K. K. Jena, S. Allauddin, R. Narayan and K. Raju, *Ind. Eng. Chem. Res.*, 2010, **49**, 4517–4527.

33 A. Santamaría-Echart, A. Arbelaitz, A. Saralegi, B. Fernández-d'Arlas, A. Eceiza and M. A. Corcuera, *Colloids Surf. A Physicochem. Eng. Asp.*, 2015, **482**, 554–561.

34 L. Lei, Z. Xia, C. Ou, L. Zhang and L. Zhong, *Prog. Org. Coat.*, 2015, **88**, 155–163.

35 Y. C. Jung and B. Bhushan, *Nanotechnology*, 2006, **17**, 4970–4980.

36 A. K. Blakney, F. I. Simonovsky, I. T. Suydam, B. D. Ratner and K. A. Woodrow, *ACS Biomater. Sci. Eng.*, 2016, **2**, 1595–1607.

37 D. E. Packham, *Int. J. Adhes. Adhes.*, 2003, **23**, 437–448.

38 L. Jiang, Y. L. Chen and C. P. Hu, *J. Coating Technol.*, 2007, **4**, 59–66.

39 H. Fu, C. Yan, W. Zhou and H. Huang, *J. Ind. Eng. Chem.*, 2014, **20**, 1623–1632.

40 T. Su, G. Y. Wang, S. L. Wang and C. P. Hu, *Eur. Polym. J.*, 2010, **46**, 472–483.

41 C. Wang, X. R. Li, B. Du, P. Z. Li, X. J. Lai and Y. H. Niu, *Colloid Polym. Sci.*, 2014, **292**, 579–587.

42 G. Gündüz and R. R. Kisakürek, *J. Dispers. Sci. Technol.*, 2004, **25**, 217–228.

43 I. Poljanšek, E. Fabjan, D. Moderc and D. Kukanja, *Int. J. Adhes. Adhes.*, 2014, **51**, 87–94.

